Comparing the Stabilities of Nanoclusters and Cluster-based Materials: Alkali Halides and the First Row Element Compounds

W. Sangthong [a,b,c], S.T. Bromley [c,d], F. Illas [c] and J. Limtrakul [a,b] *

[a] Department of Chemistry, Kasetsart University, Bangkok 10900, Thailand
[b] Center of Nanotechnology, Kasetsart University, Bangkok 10900, Thailand
[c] Departament de Química Física & Institut de Química Teòrica i Computacional (IQTCUB), Universitat de Barcelona, Cl Martí i Franquès 1, E-08028 Barcelona, Spain
[d] Institució Catalana de Recerca i Estudis Avançats (ICREA), 08010 Barcelona, Spain
E-mail: jumras.l@ku.ac.th, Tel: +662-562-5555 ext 2169, Fax: +662-562-5555 ext 2176

ABSTRACT

We present state-of-the-art plane wave periodic density functional (DF) calculations aimed to unravel the structure and electronic properties of polymorphs of LiF, BeO, BN and C obtained by assembling LiF_{12}, BeO_{12}, BN_{12} and C_{24} C_{12} building blocks with cage structure. Specifically, a nanoporous analogue of the sodalite zeolite (SOD) structure can be obtained in this way. The energy difference between the ground state phases and the SOD bulk polymorphs (per LiF, BeO, BN or C_2 unit; hereafter referred to simply as unit) was found to increase across the LiF, BeO, BN and C series with $\Delta E_{SOD\text{-}stab}$ = 0.05, 0.17, 0.68 and 1.07 eV/unit, respectively. The different electron distribution on each cluster is illustrated by the ELF analysis. The electronic properties results demonstrate that the cage-based polymorphs of these materials have band gaps significantly different from those in the most stable state phase, which could be interesting for nanotechnology applications.

Keywords: nanoclusters, sodalite, first row elements and density functional theory

1 INTRODUCTION

The appearance of pores in materials leads to a large number of applications as compared to the more dense bulk phases, zeolites being a paradigmatic example. Although experiments are now able to effectively maintain negative pressure conditions to explore the existence of phases with density lower than the ground state, this technique does not yet allow one to investigate a wide class of very low density porous crystalline materials. Nanoporous materials could be synthesized via a bottom-up route. Ultra-stable nanoclusters aggregation may result in various types of nanoporous materials. Hence, low density materials may possibly be obtained by aggregation of stable nanoclusters.

Assembling cage clusters, through edge to edge interactions, results in nanoporous materials similar to zeolites which are broadly used in industry. Recently, some of us reported on the prediction of low density nanoporous polymorphs of alkali halides [1], MgO, ZnO [2] and SiO_2 [3] based on the assembly of highly stable nanoclusters. The LiF, BeO, BN and C compounds formed from first row elements of the periodic table only provide simple models to expand the study about the stability of this type of zeolitic-like nanoporous materials.

Rock salt is the ground state phase of highly ionic LiF whereas BeO crystallizes in a wurtzite structure. Hexagonal structures are found to be stable in BN and C also appears in the form of graphite. In the present work, we report DF calculations aimed to study the geometry and electronic structure of the LiF_{12}, BeO_{12}, BN_{12} and C_{24} cage clusters of first row elements and to explore the stability of the new low density phases formed by assembling these building blocks relative to the ground state phase.

2 COMPUTATIONAL DETAILS

Two sets of plane wave density functional calculations have been carried out to explore the possibility of low density phases of the binary compounds of the first row elements (LiF, BeO, BN) and of C. The first one involves the stability of the LiF_{12}, BeO_{12} BN_{12} and C_{24} cage clusters, whereas the second one concerns extended bulk systems built from these units. Energies, structures, and electronic states of cluster isomers and bulk phases of these compounds were calculated using the PW91 exchange-correlation potential [4-5] and the VASP code [6-8]. The PAW method [9] was used to represent the effect of the atomic cores and a 415 eV energy cutoff was used for the plane wave expansion. For the discrete systems, a large enough box has been constructed so that the distance between repeated clusters is larger than 1 nm. For the solids, the unit cell is defined by the crystal structure. The integrations in the reciprocal space is accomplished by using Monkhorst-Pack grids of special *k* points (7×7×7 for rock salt, wz, BN and graphite, 3×3×3 for low dense phases and Γ point for isolated clusters). For bulk phases the volume versus energy data was fitted using the Birch-Murnaghan EOS [10].

3 RESULTS & DISCUSSION

3.1 Stability of $(AB)_{12}$ cage clusters

The main purpose of the present work is to analyze the possible existence of low density bulk phases of the first row element binary compounds and their relative stability

with respect to the ground state phases. First, we analyze the possible structure of LiF_{12}, BeO_{12}, BN_{12} and C_{24} cage clusters consisting of 6 square faces and 8 hexagons. The geometry of these cage clusters is shown in Figure 1 and the optimized parameters are reported in Table 1.

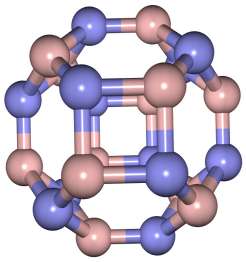

Figure 1: Geometry of LiF_{12}, BeO_{12} and BN_{12} cage clusters.

The geometry of these cage clusters is shown in Figure 1 and the optimized parameters are reported in Table 1.

Parameters	LiF	BeO	BN	C
d (sq-hex), Å	0.168	0.159	0.149	0.149
d (hex-hex), Å	0.163	0.153	0.144	0.138
∠ABA (sq),°	95.0 (Li)	98.3 (Be)	98.4 (B)	90.0
	84.9 (F)	80.8 (O)	80.3 (N)	90.0
∠ABA (hex), °	122.0 (Li)	124.9 (Be)	125.8 (B)	120.0
	117.4 (F)	112.4 (O)	110.9 (N)	120.0
LUMO, eV	-0.87	-1.22	-1.48	-3.89
HOMO, eV	-7.72	-6.96	-6.46	-5.10
E. Gap, eV	6.85	5.74	4.98	1.21
E./unit, eV	-9.28	-13.44	-16.24	-16.28

Table 1: Structural parameters and electronic features of the LiF_{12}, BeO_{12}, BN_{12} and C_{24} cage clusters.

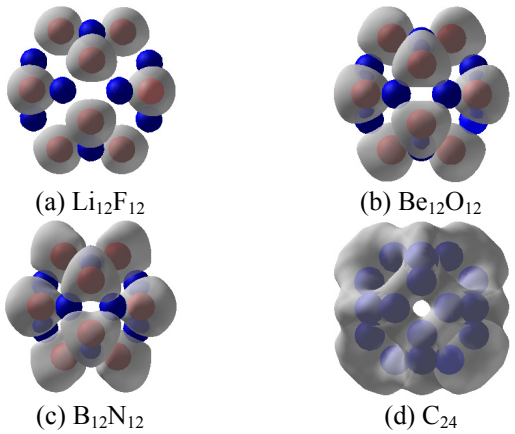

(a) $Li_{12}F_{12}$ (b) $Be_{12}O_{12}$

(c) $B_{12}N_{12}$ (d) C_{24}

Figure 2: Electron density map of LiF_{12}, BeO_{12}, BN_{12} and C_{24} cage clusters.

The geometry optimization results in a slight deviation of the molecular structure from a regular configuration except for the C24 cluster. These deviations result from charge transfer and ionicity in the chemical bond of the heteroatomic clusters. The bond distances increase with increasing ionicity. Bond angles are slightly different from the expected regular value because of the inhomogeneous electron localization. The energy gap, ΔE, between the HOMO and the LUMO and energy per unit for all cage clusters decreases from LiF to C.

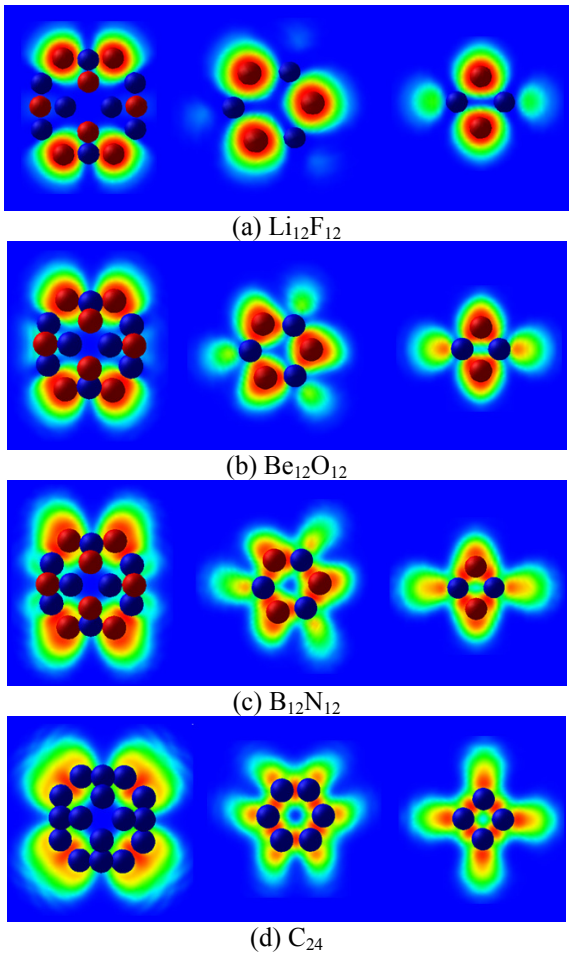

(a) $Li_{12}F_{12}$

(b) $Be_{12}O_{12}$

(c) $B_{12}N_{12}$

(d) C_{24}

Figure 3: Electron density maps in the three planes passing through $(AB)_{12}$ cage clusters.

To obtain additional detailed insight into the bonding and ionic polarization in the cage clusters, we have also analyzed the changes in the electronic structure upon increasing the formal cation/anion radii ratio using the Electron Localization Function (ELF). In the case of the first row element clusters, the chemical bonding is highly ionic in LiF and decreases when moving to C. From the ELF maps shown in Figure 2 one can note that when going from the extremes of LiF to CC, through BeO and BN as intermediate cases, interesting changes emerge. The ELF maps for the LiF cluster show rather spherical ELF basins, which are indicative of a highly ionic character, and they are increased and noticeably deformed when going from heteroatomic cages LiF, BeO, BN

to the case of C. In fact, for the carbon cage cluster the situation is rather different, the ELF maps are largely deformed from the symmetric spherical shape, the electron pair are clearly distributed all around the cluster. This is a clear indication that, in spite of a similar structure, the chemical bond between atoms in cage clusters is different, as expected, from chemical intuition.

A clear difference exists in the chemical bond of the first row element cage structures, which is further confirmed by the ELF maps in each plane reported in Figure 3

3.2 Relative stability of the sodalite phase

In order to compare the stability of the sodalite phase to that of the most stable polymorph and other possible phases, we explicitly considered other phases and determined the optimized parameters using the Birch-Murnaghan EOS. From the optimized parameters reported in Table 3 we find that the optimized volume per unit of the sodalite phase is larger than that of the ground state phase of LiF and BeO by 53% and 20%, respectively, whereas for for BN and C the volume of the most stable phase per unit is larger than that of the sodalite phase by 38% and 35%, respectively.

Phase-AB	E0	ΔE0	V0	B0
RS-LiF (exp)			16.32[a]	69.9[b]
RS-LiF (present work)	-9.73	0.00	16.85	68.6
SOD-LiF	-9.68	0.05	25.87	41.7
WZ-BeO (exp)[c]	-12.73		13.79	212
WZ-BeO (present work)	-14.38	0.00	14.02	210.4
SOD-BeO	-14.21	0.17	17.05	168.34
HEX-BN (exp)[d]				36.7
HEX-BN (present work)	-17.67	0.00	19.37	39.82
SOD-BN	-16.99	0.68	14.61	290.05
Graphite-C (exp)[e]			35.15	42
Graphite-C (exp)[f]			35.12	33.8
Graphite-C (present work)	-18.49	0.00	18.98	39.01
SOD-C	-17.42	1.07	14.04	328.41

[a] Ref. 11, [b] Ref. 12, [c] Ref. 13, [d] Ref. 14, [e] Ref. 15, [f] Ref. 16

Table 2: Properties for various polymorphs (per unit) of LiF, BeO, BN and C as calculated from the EOS fits to the GGA-DFT calculated data: E0 is the minimum total energy (eV), ΔE_0 the total energy differences (eV), V0 the volume at minimum energy ($Å^3$) and B0 the bulk modulus (GPa). V0 and B0 are compared with available experimental values.

In order to find the trend on the stability of the sodalite phase relative to the other phases considered in the present work, we plot in Figure 4 the energy difference (per unit) between the total energy of sodalite and the total energy of the most stable polymorph. From Figure 4 a clear monotonous trend is observed which makes it undoubtedly clear that the stability of the sodalite phase decreases along the LiF, BeO, BN and C series or that increasing covalent character of the chemical bond destabilizes the low density polymorph with respect to the more dense phases corresponding to the most stable polymorph. These results indicate that the sodalite form is likely to be easily synthesized from highly ionic compounds where for the remaining studied systems this will face increasing difficulties.

3.3 Electronic properties

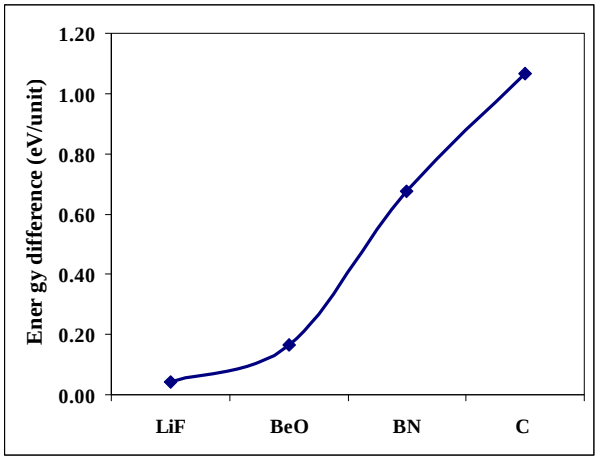

Figure 4: The energy differences between the sodalite phase and the ground state phase.

In order to investigate the electronic structures of the different polymorphs of LiF, BeO, BN and C more precisely, we have calculated the total density of states using the standard procedure. All band energies are given with respect to the Fermi energy (E_F) and shown in Figure 5. The Fermi energy is located at the top of the valence bands which is located at the Γ point and is set to zero. The DOS plots for rock salt and sodalite phases of LiF are presented in Figures 5a1 and 5a2, respectively. Below zero, there is a broad range of F states below the top of the valence band, whereas the conduction band consists of F and Li states. The difference between the maximum of the F valence band and the minimum of the Li conduction band results in a band gap of 8.83 eV and 6.36 eV for rock salt and sodalite phases, respectively. The band gap for the rock salt phase is underestimated with respect to the experimental value of 13.6 eV. This is a well known failure of the GGA functional. Nevertheless, one expects that the relative trends are well reproduced. The DOS plots of BeO for wurtzite and sodalite phases (Figures 5b1 and 5b2) display the same trend, the valence regions are mainly composed of O states while the conduction bands originate predominantly from Be states. The calculated energy gaps are 7.22 eV and 5.18 eV for wurtzite and sodalite phases, respectively. Again the band gap for wurtzite is underestimated with respect to the experimental value of 10.6 eV. The DOS for the two polymorphs of BN phases are reported in Figures 5c1 and 5c2 and also show that the top and the low energy part of the valence band is predominantly formed by the states of nitrogen atoms. The upper conduction band is dominated by contributions from both B and N states. The calculated band gap for hexagonal BN is 4.37 eV (experimental value = 5.4 eV) while the

calculated value for the sodalite phase is 4.38 eV. For the graphite phase (Figure 5d1), the DOS for the unit cell shows two groups of peaks with a band gap of 1.43 eV between them. The Fermi energy is placed at the top of the valence band (VB) so all states below it have two electrons per orbital, and all states above it are unoccupied. The energy gap of the sodalite form of carbon is calculated to be 2.44 eV.

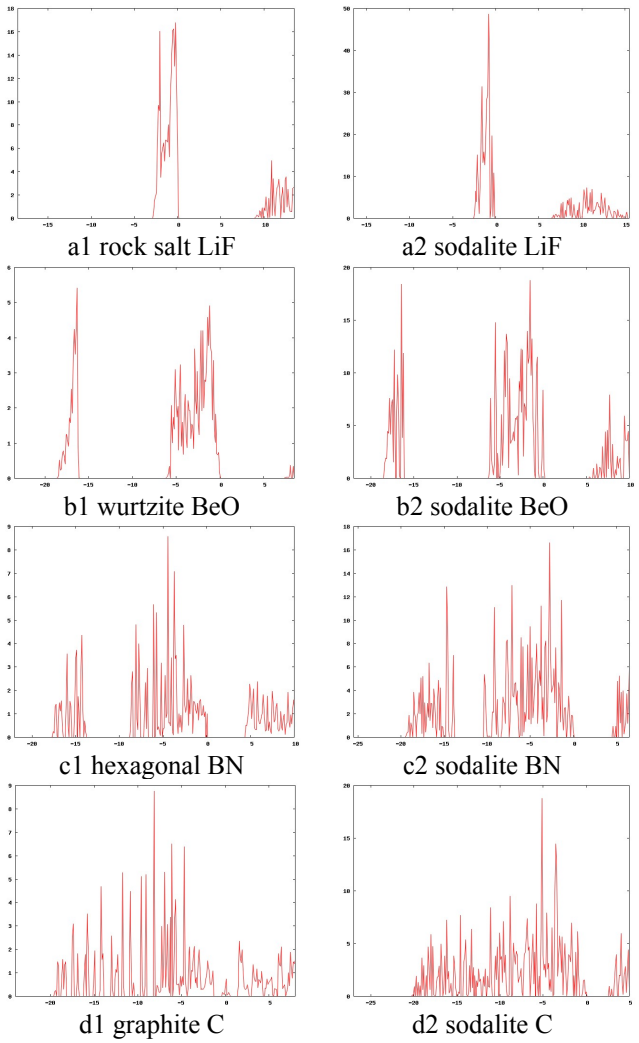

Figure 5: Total density of states of bulk phases of LiF, BeO, BN and C.

4 CONCLUSION

A bottom up approach and state-of-the-art plane wave periodic density functional calculations were utilized to investigate the possible existence of low density phases of the LiF, BeO, BN first row element binary compounds and of C. The existence of stable $(AB)_{12}$ or C_{24} cage clusters, where AB= LiF, BeO, BN, suggest that these could act as building blocks to form novel nanoporous materials. The calculated HOMO-LUMO gaps of all clusters decreases along the LiF, BeO, BN, C series and can be understood from the ELF analysis. In fact, the ELF analysis of the bare cage clusters explains the difference in optimized geometry and electron distribution on each cluster. Bulk materials constructed from the cages may exhibit a sodalite structure; the total energy difference (per unit) between the most stable and the sodalite polymorphs was found to increase when going from LiF to C ($\Delta E_{SOD\text{-}stab}$=0.05, 0.17, 0.68, 1.07 eV/unit for LiF, BeO, BN and C, respectively). The calculated HOMO-LUMO gaps and electronic structure of all predicted nanoporous phases are different from those of the corresponding ground state phases. Merging state of the art density functional calculations and a bottom-up strategy provides a complementary way to motivate further synthesis and applications of new predicted nanoporous phases.

ACKNOWLEDGEMENTS

This work was supported in part by grants from the National Science and Technology Development Agency (NSTDA), KURDI the Thailand Research Fund (to WS. and JL.) and the Commission on Higher Education, Ministry of Education under Postgraduate Education and Research Programs in Petroleum and Petrochemicals, and Advanced Materials. This study has been supported in part by the Spanish Ministerio de Ciencia e Innovacion grant FIS2008-02238/FIS.

REFERENCES

[1] W. Sangthong, J. Limtrakul, F. Illas and S. T. Bromley, J. Mater. Chem., 2008, 18, 5871.
[2] J. Carrasco, F. Illas and S. T. Bromley, Phys. Rev. Lett., 2007, 99, 235502.
[3] J. C. Wojdel, M. A. Zwijnenburg and S. T. Bromley, Chem. Mater., 2006, 18, 1464.
[4] J. P. Perdew, J. A. Chevary, S. H. Vosko, K. A. Jackson, M. R. Pederson, D. J. Singh and C. Fiolhais, Phys. Rev. B, 1992, 46, 6671.
[5] J. A. White and D. M. Bird, Phys. Rev. B, 1994, 50, 4954.
[6] G. Kresse and J. Hafner, Phys. Rev. B, 1993, 47, 558.
[7] G. Kresse and J. Furthmu¨ ller, Comput. Mater. Sci., 1996, 6, 15.
[8] G. Kresse and J. Furthmu¨ ller, Phys. Rev. B, 1996, 54, 11169.
[9] P. E. Blöchl, Phys. Rev. B, 1994, 50, 17953.
[10] F. Birch, Phys. Rev., 1947, 71, 809.
[11] V. A. Streltsov, V. G. Tsirelson, R. P. Ozerov and O. A. Golovanov, Kristallografiya, 1987, 33, 90.
[12] C. V. Briscoe and C. F. Squire, Phys. Rev., 1957, 1175, 106.
[13] Hazen R M and Finger L W, J. Appl. Phys., 1986, 59, 3728.
[14] S. Bohr, R. Haubner, B. Lux, Diamond Relat. Mater., 1995, 4, 714.
[15] Y.X. Zhao and I.L. Spain, Phys. Rev. B, 1989, 40, 993.
[16] M. Hanfland, H. Beister, and K. Syassen, Phys. Rev. B, 1989, 39, 12 598.